The EMBO Journal Vol.18 No.23 pp.6762–6770, 1999

Interaction of agrin with laminin requires a coiled-coil conformation of the agrin-binding site within the laminin γ1 chain

Richard A.Kammerer, Therese Schulthess, Ruth Landwehr, Beat Schumacher[1], Ariel Lustig, Peter D.Yurchenco[2], Markus A.Ruegg[1], Jürgen Engel[3] and Alain J.Denzer[1]

Departments of Biophysical Chemistry and [1]Pharmacology, Biozentrum, University of Basel, Klingelbergstrasse 70, CH-4056 Basel, Switzerland and [2]Department of Pathology and Laboratory Medicine, Robert Wood Johnson Medical School, Piscataway, NJ 08854, USA

[3]Corresponding author
e-mail: engel@ubaclu.unibas.ch

Coiled-coil domains are found in a wide variety of proteins, where they typically specify subunit oligomerization. Recently, we have demonstrated that agrin, a multidomain heparan sulfate proteoglycan with a crucial role in the development of the nerve–muscle synapse, binds to the three-stranded coiled-coil domain of laminin-1. The interaction with laminin mediates the integration of agrin into basement membranes. Here we characterize the binding site within the laminin-1 coiled coil in detail. Binding assays with individual laminin-1 full-length chains and fragments revealed that agrin specifically interacts with the γ1 subunit of laminin-1, whereas no binding to α1 and β1 chains was detected. By using recombinant γ1 chain fragments, we mapped the binding site to a sequence of 20 residues. Furthermore, we demonstrate that a coiled-coil conformation of this binding site is required for its interaction with agrin. The finding that recombinant γ1 fragments bound at least 10-fold less than native laminin-1 indicates that the structure of the three-stranded coiled-coil domain of laminin is required for high-affinity agrin binding. Interestingly, no binding to a chimeric γ2 fragment was observed, indicating that the interaction of agrin with laminin is isoform specific.

Keywords: agrin/coiled-coil domain/extracellular matrix/laminin isoforms/protein–protein interactions

Introduction

The α-helical coiled coil is probably the most widespread subunit oligomerization motif found in proteins (Lupas, 1996; Kammerer, 1997). This protein structure consists of 2–5 right-handed amphipathic α-helices that 'coil' around each other in a left-handed supertwist (Crick, 1953; O'Shea *et al*., 1991). The protein sequences of coiled coils are characterized by a heptad repeat of seven residues denoted **a**–**g**, with a 3,4-hydrophobic repeat of mostly apolar amino acids at positions **a** and **d** (Sodek *et al*., 1972; McLachlan and Stewart, 1975; Cohen and Parry, 1990). Coiled-coil proteins fulfill a variety of biological functions (Lupas, 1996; Kammerer, 1997). In several families of transcriptional activators, for example, short coiled coils mediate dimerization and the combinatorial arrangement of factors by selective heterodimerization (in bZip proteins), position the DNA-binding regions on DNA and even bind to the DNA themselves (in serum response factor; Landschulz *et al*., 1988; Alber, 1992).

Laminins are major extracellular glycoproteins composed of three different polypeptide chains α, β and γ. Chain selection and association into native molecules is mediated by an extended three-stranded coiled-coil domain leading to asymmetric heterotrimers. To date, 11 genetically distinct laminin chains (α1–α5, β1–β3 and γ1–γ3) and 12 different isoforms (laminins-1 to -12) have been reported (Timpl and Brown, 1994; Maurer and Engel, 1996; Miner *et al*., 1997; Koch *et al*., 1999). The existence of multiple chains that oligomerize with a defined stoichiometry provides a means to generate functional diversity. In higher vertebrates, laminins play essential roles. Several lines of evidence indicate that these proteins are crucial structural elements forming one of the two self-assembling and independent networks of basement membranes; the other one is composed of collagen IV (Yurchenco and Cheng, 1993; Yurchenco and O'Rear, 1994). Linkage of the two distinct networks via nidogen/entactin provides a primary scaffold to which other glycoproteins and proteoglycans such as perlecan attach (for review, see Yurchenco and O'Rear, 1994). Furthermore, laminins interact with cell surface receptors such as α-dystroglycan, a member of the large dystrophin glycoprotein complex, and the integrins. These interactions attach cells to the extracellular matrix and propagate morphogenetic information to the cell's interior (for review, see Timpl and Brown, 1994; Clark and Brugge, 1995; Henry and Campbell, 1996). The distinct molecular composition of basement membranes is thought to be important for these processes.

Recently, we have demonstrated that agrin, a large multidomain heparan sulfate proteoglycan essential for synapse formation at the neuromuscular junction (for review, see McMahan, 1990; Denzer *et al*., 1996), binds to laminin-1 (Denzer *et al*., 1997, 1998). This high-affinity interaction (K_d ~5 nM) is mediated by the N-terminal domain of agrin (NtA) and appears to be required for the localization of the molecule to the synaptic basal lamina at the nerve–muscle contact and other basement membranes (Denzer *et al*., 1995, 1997, 1998). Biochemical and electron microscopic data indicated that agrin binds near to the center of the laminin-1 coiled-coil. This region extends from the cysteine-rich loop α to the N-terminus of the E8 fragment (Figure 1; Denzer *et al*., 1998).

Besides the binding of agrin to laminin, only a few interactions between coiled coils and other protein struc-

tures have been described in the literature. To our knowledge, no detailed description of this type of interaction exists. Therefore, a detailed characterization of a coiled-coil–non-coiled-coil interaction should be of particular importance as it assigns a novel function besides oligomerization to coiled-coil domains. Here we characterize the agrin-binding site in the central region of the coiled-coil domain of laminin-1 in detail. We have addressed the requirement of individual laminin-1 subunits for the agrin–laminin-1 interaction by transfecting COS cells with cDNAs coding for full-length α1, β1 and γ1 chains. We demonstrate that the γ1 subunit is sufficient to mediate specific binding to the NtA domain of agrin. These results were corroborated with recombinant coiled-coil polypeptide chain fragments produced by heterologous gene expression in *Escherichia coli*. Furthermore, by deletion mapping, we located the agrin-binding site within laminin γ1 to a sequence of 20 residues. Notably, a coiled-coil conformation of this site is required for its binding to the NtA domain. No significant binding of the homologous amino acid sequence from laminin γ2 was found, suggesting that the distinct molecular composition of basement membranes specifies intercellular interactions.

Results

Specific binding of agrin to recombinant laminin γ1 chains

We have reported previously that agrin binds to a central region within the coiled-coil domain of laminin-1, which spans ~130 residues in each subunit (shaded region A shown in Figure 1; Denzer *et al*., 1998). Accordingly, one, two or all three subunits may be involved in the interaction with agrin. In order to address the subunit requirement of this interaction, we individually expressed full-length laminin α1, β1 and γ1 polypeptide chains in COS cells. The binding activities of individual laminin chains were tested by using the fragment cN25Fc, which is a chimera comprising the NtA domain and the first follistatin-like domain of agrin, and the constant region of a mouse IgG (Denzer *et al*., 1997). Because β1 and γ1 subunits are not secreted (Yurchenco *et al*., 1997),

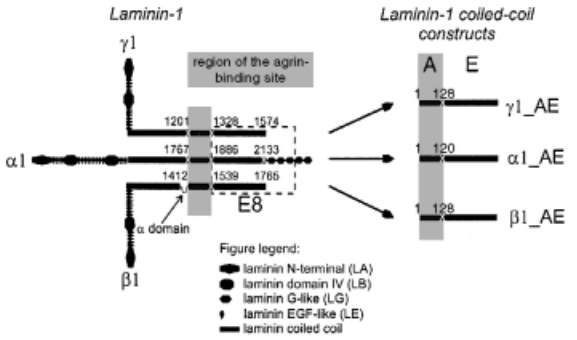

Fig. 1. Schematic representation of the domain organization of laminin-1 and recombinant coiled-coil fragments used in this study. Domain symbols and designations are according to Bork and Bairoch (1995). Amino acid positions of the agrin-binding region (shaded area; Denzer *et al*., 1998), the elastase-derived fragment E8 and the cysteine-rich α-domain within the β1 subunit are indicated according to the numbering of Sasaki and Yamada (1987) and Sasaki *et al*. (1987, 1988). A, agrin-binding region; E, E8 sequence.

transfected cells were fixed and permeabilized to allow cN25Fc to penetrate the cell membrane and to interact with the intracellular pool of recombinant laminin chains. The binding of cN25Fc to laminin polypeptide chains was visualized by immunostaining using a first antibody recognizing the IgG part of the chimeric fragment. In contrast to cells transfected with the laminin α1 or β1 subunits, intracellular staining was observed for cells expressing the recombinant γ1 chain (Figure 2A). The binding of cN25Fc to the γ1 subunit was inhibited by co-incubation with the bacterially expressed coiled-coil fragment γ1_AE (Figure 1), indicating a specific interaction between the two components (Figure 2A). As the failure to observe binding to laminin α1 and β1 subunits could potentially result from low-level expression of the proteins, Western blot analysis was performed. Analysis of transfected cells using anti-laminin antibodies revealed, however, that comparable amounts of each full-length subunit were synthesized (Figure 2B). Notably, the apparent molecular masses of all three recombinant full-length polypeptide chains were reduced compared with those of the constituent chains from purified laminin-1 (e.g. 400 kDa band for α1, 220 kDa band for β1, and 200 kDa band for γ1), suggesting different glycosylation of the recombinant polypeptides (Figure 2B). Furthermore, Western blot analysis of cells transfected with laminin γ1 revealed additional bands, which probably correspond to degradation products.

To confirm our findings that the laminin γ1 subunit is sufficient to mediate specific binding to agrin and to exclude the possibility of interference by endogenous laminin expressed by COS cells, we performed solid-phase radioligand-binding assays with purified proteins and recombinant polypeptide chain fragments produced in *E.coli*. Fragments α1_AE, β1_AE and γ1_AE were designed, which comprise those sequences of the laminin-1 coiled-coil domain downstream from loop α that contain the agrin-binding region (Figure 1). Full-length chicken agrin (cAgrin; Denzer *et al*., 1995) was immobilized on microtiter plates and incubated with 8 nM iodinated laminin-1 in the presence of 10 mM EDTA to prevent network formation by the self-assembly of laminin molecules (Yurchenco and Cheng, 1993). To inhibit the binding of [^{125}I]laminin-1 to cAgrin, either 500 nM laminin-1 or 1 μM recombinant coiled-coil polypeptide chain fragments were included during incubation. As expected, only unlabeled laminin-1 and γ1_AE inhibited the interaction of iodinated laminin-1 with agrin (Figure 2C), which is consistent with the results obtained in COS cells (Figure 2A). Consistent results were also obtained when α1_AE, β1_AE or γ1_AE were immobilized on microtiter plates and the binding of [^{125}I]cAgrin was competed with purified laminin-1 (data not shown). The finding that the inhibition with γ1_AE was only partial may be explained in terms of a lower agrin-binding affinity of single γ1 chains compared with native laminin-1 and/or the presence of an additional laminin-1-binding site within agrin. To address the first possibility, maximal inhibition of the competitor was measured. As shown in Figure 3, maximal response was reached at a γ1_AE concentration of 10 μM. Dose–response measurements in which γ1_AE was immobilized and incubated with iodinated agrin further supported our finding that the

binding affinities of individual γ1 subunits are significantly lower than for laminin-1 (data not shown). The residual fraction of bound laminin-1 (~20%) at γ1_AE concentrations of maximal inhibition (Figure 3) indicates that agrin probably also contains an additional laminin-binding site. As this binding could be inhibited efficiently by heparin (data not shown), the most likely candidates for such an interaction are the heparan sulfate glycosaminoglycan side chains of agrin.

Taken together, our findings demonstrate that the laminin γ1 subunit contains a sequence of maximally 128 residues within its coiled-coil domain that is sufficient for the specific interaction with agrin.

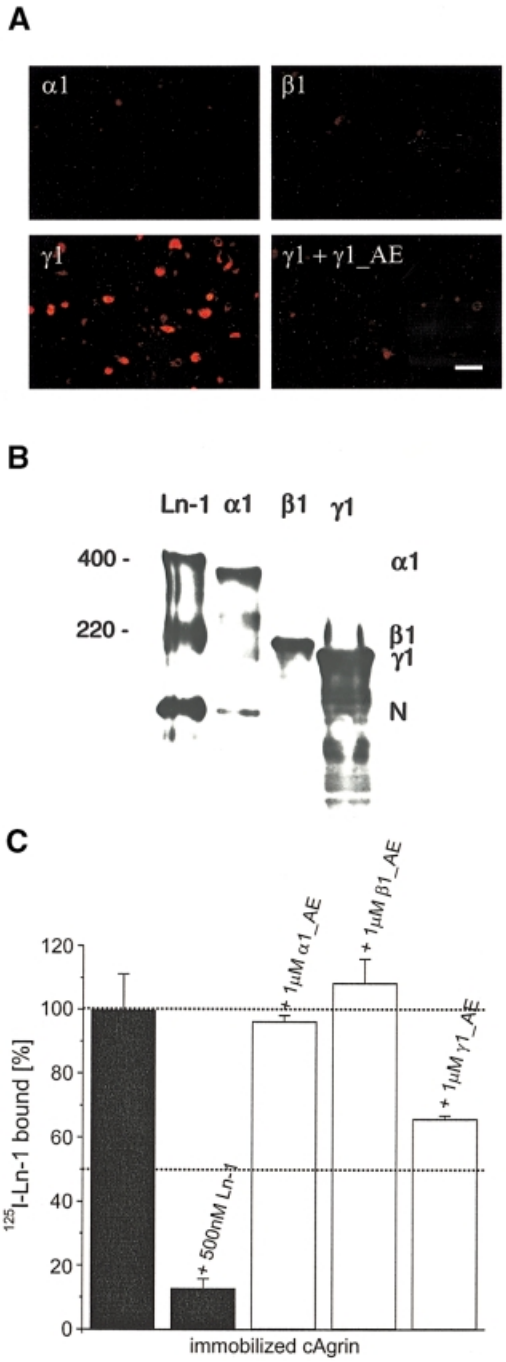

Mapping of the agrin-binding site within the laminin γ1 coiled-coil domain

To locate the agrin-binding site precisely within the laminin coiled-coil domain, we produced a number of γ1 chain fragments by successive removal of residues from the N-terminus of γ1_AE (Figure 4A) and assessed their ability to bind to agrin by solid-phase radioligand-binding assays. As depicted in Figure 4B, deletion of >95 residues from γ1_AE completely abolished binding activity, indicating that residues downstream of amino acid 95 are necessary for the interaction with agrin. Based on this result, we next focused our attention on the remaining 33 C-terminal residues of the agrin-binding region.

First, we designed a γ1 chain variant, γ1_A, in which the E8 part was deleted. This fragment corresponds to the 128 residues of the agrin-binding region (Figure 5A) but contains a C-terminal Gly-Gly-Cys extension to stabilize an eventual coiled-coil structure by intermolecular disulfide bond formation. Complete loss of binding activity was observed for this fragment (data not shown). This rather unexpected result prompted us to hypothesize that the E8 part of the fragments derived from γ1_AE induces a coiled-coil conformation within the binding site, which is required for the interaction with agrin. Indeed, our hypothesis was supported by CD spectroscopy and analytical ultracentrifugation analysis of γ1_ΔN95AE, the shortest fragment with binding activity, and the γ1_A peptide (Figure 5A). The CD spectra recorded from γ1_ΔN95AE and γ1_A were characteristic for α-helical proteins with minima near 208 and 222 nm (Figure 5B). The thermal stability of the two fragments was assessed by temperature-induced denaturation profiles recorded by CD at 221 nm. γ1_ΔN95AE exhibited a profile with a sigmoid shape typical for coiled coils, which was monophasic and reversible, with >90% of the starting signal regained upon cooling (Figure 5C). However, the thermal stability of γ1_ΔN95AE was relatively low as revealed by its midpoint of thermal unfolding (T_m) at ~25°C. In contrast, the thermal melting profile recorded from γ1_A showed a broad, non-cooperative transition

Fig. 2. Specific binding of agrin to recombinant laminin-1 full-length chains and fragments. (**A**) Binding of 45 nM cN25Fc to individual full-length laminin-1 chains expressed in transiently transfected COS cells was visualized by intracellular immunofluorescence staining using a first antibody recognizing the IgG portion of the chimeric agrin fragment. Binding was only observed in cells transfected with the γ1 chain (γ1). The binding of cN25Fc to the laminin γ1 chain could be inhibited by competition with 10 μM of the recombinant coiled-coil fragment γ1_AE (γ1 + γ1_AE), demonstrating the specificity of this interaction. Bar, 150 μm. (**B**) Western blot of mouse laminin-1 (Ln-1) or total proteins of COS cells transfected with the cDNAs coding for individual laminin-1 subunits (α1, β1 and γ1) after separation by 3–12% SDS–PAGE under reducing conditions and transfer to nitrocellulose. Laminin α1 (400 kDa), β1 (220 kDa) and γ1 (200 kDa) chains were detected with an antiserum raised against the mouse laminin-1–nidogen complex. Comparable amounts of each chain were produced by the transfected cells. N, nidogen. (**C**) Inhibition of the binding of radiolabeled laminin-1 to agrin by unlabeled laminin-1 or bacterially expressed coiled-coil fragments monitored by solid-phase radioligand-binding assays. Full-length agrin was immobilized on microtiter plates and incubated with 8 nM [^{125}I]laminin-1 in the presence or absence of competitors. Each value is the mean ± SD of three measurements and represents binding after subtraction of the counts to BSA-coated wells (3.7 ± 0.4% of the total laminin-1 binding).

Table I. Sedimentation coefficients ($s_{20,w}$) and average molecular masses of recombinant polypeptide chain fragments

Fragment	$s_{20,w}$ (S)	Molecular mass (kDa)	
		Observed	Calculated[a]
γ1_A	1.58	32	30.4[b]
γ1_A (RA)	1.32	13.8	15.2
β1_A	2.47	63 ± 3	30.7[b]
β1_A (RA)	1.95	30.6	15.4
α1_A	2.9	70 ± 3	14.3
γ1_ΔN95AE	3.0	62 + 79[c] 32 + 83[c]	62.2[b]
γ1_ΔN95AE (RA)	2.3	35 + 84[c] 67	31.1
γ1_GΔN93AEΔC219	1.55	25.4	10.6

All fragments were analyzed at 20°C in 5 mM sodium phosphate buffer (pH 7.4) containing 150 mM sodium chloride.
[a]Molecular mass of the monomer based on its amino acid sequence.
[b]Molecular mass of the disulfide-linked dimer based on its amino acid sequence.
[c]Non-homogeneous molecular mass distributions were observed. The lower number is the minimum weight average near the meniscus and the second number is an estimate for the weight average near the bottom of the cell.
RA, reduced and alkylated.

(Figure 5C). Consistent results were also obtained with γ1_ΔN95AE and γ1_A fragments in which the C-terminal Cys sulfhydryl group had been alkylated with *N*-ethylmaleimide (data not shown).

The oligomeric state of the recombinant proteins was assessed by analytical ultracentrifugation (Table I). Sedimentation equilibrium of disulfide-linked and alkylated γ1_ΔN95AE yielded average molecular masses indicative of a mixture of oligomerization states, which is consistent with the thermal instability of the polypeptide chain fragments as well as the degree of α-helicity of only ~50%. The sedimentation equilibrium profile suggested that at 20°C and a total chain concentration of 5 μM (the conditions used in the inhibition assays), the protein is present predominantly in an aggregated form. For disulfide-linked and alkylated γ1_A peptides, molecular masses corresponding to dimers and monomers, respectively, were obtained. Based on these findings, we concluded that isolated γ1_ΔN95AE, in contrast to γ1_A, forms relatively unstable coiled-coil structures. It should be noted that similar results were also obtained with the γ1_ΔN110AE fragment (data not shown) for which no agrin-binding activity was observed. These findings suggest that the oligomerization specificity of the N-terminally truncated γ1 fragments resides within their E8 region.

Based on the above findings, we could not exclude the possibility that the lack of agrin binding observed for individual α1 and β1 full-length chains (Figure 2A) and chain fragments (Figure 2C) is due to a loss of structure of the binding site. Thus, and because the α1_AE fragment was not suitable for structural characterization due to its low solubility, we produced the recombinant α1_A and β1_A polypeptide chain fragments, which, according to their electron microscopic localization (Denzer *et al.*, 1998; Figure 1), are candidates for an agrin-binding site. The structures of α1_A and both disulfide-linked and alkylated β1_A differ from that of the γ1_A peptide. In

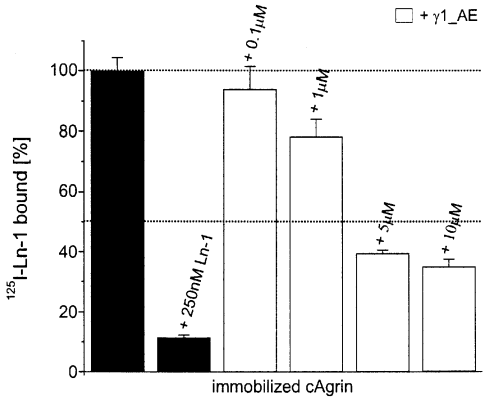

Fig. 3. Concentration-dependent inhibition of the laminin–agrin interaction by the recombinant laminin γ1_AE coiled-coil fragment. Maximal inhibition of the binding of 8 nM [^{125}I]laminin-1 to immobilized full-length agrin was reached with 10 μM γ1_AE. Note that 250 nM of unlabeled laminin-1 were sufficient for complete inhibition, indicating that the binding of agrin to the individual γ1 chain fragment is of significantly lower affinity. Values represent the mean ± SD of three measurements after subtraction of the background signal (BSA-coated wells). Background values were 9.2 ± 0.3% of total laminin-1 binding.

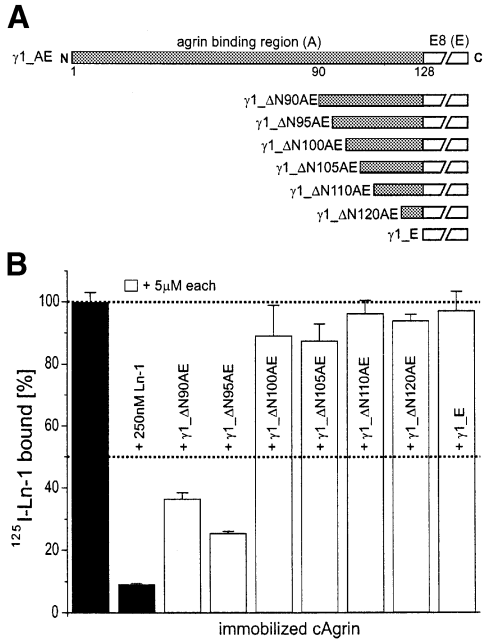

Fig. 4. Localization of the N-terminal boundary of the agrin-binding site on laminin γ1. (**A**) Schematic representation of the N-terminally truncated laminin γ1 fragments used in the solid-phase radioligand-binding assay. The agrin-binding region (A; shaded) and the E8 sequence (E; white) are indicated. (**B**) Solid-phase radioligand-binding assay. Unlabeled laminin-1 efficiently inhibited the binding of 8 nM [^{125}I]laminin-1 to immobilized full-length agrin. Complete loss of inhibition activity was observed for γ1 coiled-coil fragments in which >95 N-terminal residues of the agrin-binding region were removed. Values are the mean ± SD of one representative experiment with two independent measurements after subtraction of the background signal (BSA-coated wells; 5.1 ± 0.3% of total laminin-1 binding).

contrast to γ1_A (Figure 5C; Table I), α1_A and disulfide-linked and alkylated β1_A folded into homotypic coiled-coil structures, as shown by their helical content, their reversible CD unfolding profiles and their oligomerization states (Table I). At 5°C and a chain concentration of 10 μM, the fragments were ~60–70% helical and revealed

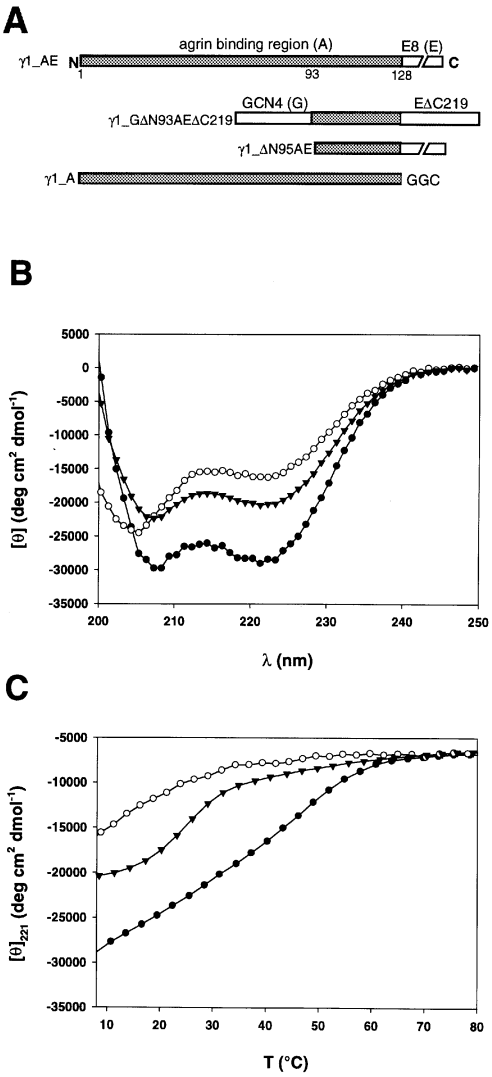

Fig. 5. (**A**) Recombinant γ1 fragments analyzed by CD spectroscopy. (**B**) Far-UV CD spectra recorded from γ1_A (○), γ1_ΔN95AE (▲) and γ1_GΔN93AEΔC219 (●) at 5°C. Polypeptide chain concentrations were 35 μM in 5 mM sodium phosphate buffer (pH 7.4) containing 150 mM sodium chloride. The spectra are characteristic of α-helical proteins with minima near 208 and 222 nm. (**C**) Temperature-induced unfolding profiles of the recombinant polypeptide chain fragments (same symbols) monitored by the change of the CD signal at 222 nm. Peptide concentrations and buffer conditions were as in (B).

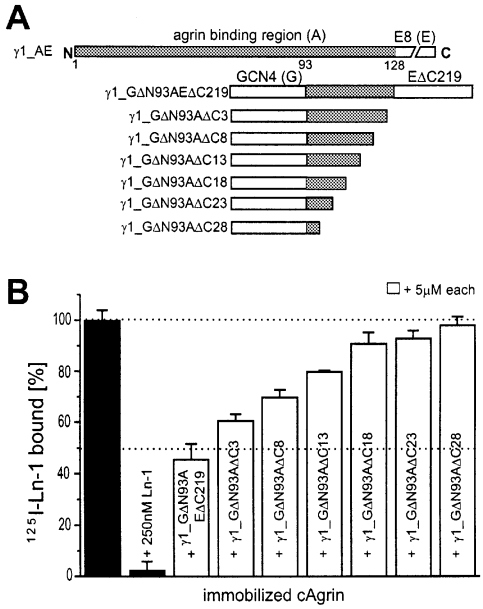

Fig. 6. Localization of the C-terminal boundary of the agrin-binding site on laminin γ1. (**A**) Schematic representation of the chimeric γ1 peptides. In-register heptad repeat fusion to the C-terminus of the dimeric GCN4 leucine zipper (G; white) was used to trigger coiled-coil formation of the γ1 fragments (A; shaded). (**B**) Binding activities of the chimeric coiled-coil fragments analyzed by solid-phase radioligand-binding assays. Only peptides in which ⩽13 residues were removed from the C-terminus revealed partial inhibition of the binding of 8 nM [^{125}I]laminin-1 to immobilized full-length agrin. Each value is the mean ± SD of three measurements of one representative experiment after subtraction of the background value (BSA-coated wells; 6.7 ± 0.4% of total laminin-1 binding).

T_ms at ~30°C (data not shown). Analytical ultracentrifugation sedimentation equilibrium measurements yielded average molecular masses that are consistent with pentameric, tetrameric and dimeric structures of α1_A, disulfide-linked β1_A and alkylated β1_A, respectively (Table I). The fragments were inactive in competition or solid-phase binding assays (data not shown), demonstrating that the coiled-coil property of laminin chains alone is not sufficient for the interaction with agrin.

To challenge further our hypothesis that the agrin-binding site requires a coiled-coil conformation for activity, coiled-coil formation of the 33 C-terminal residues of the agrin-binding region was 'triggered' by in-register heptad repeat fusion to the C-terminus of the dimeric leucine zipper from the yeast transcriptional activator GCN4 (Figure 6A; Landschulz *et al.*, 1988). This chimeric polypeptide chain fragment, γ1_GΔN93AEΔC219 (Figure 5A), had features characteristic of a two-stranded coiled coil as revealed by its high degree of α-helicity (Figure 5B), high thermal stability (Figure 5C), analytical ultracentrifugation sedimentation velocity profiles and sedimentation equilibrium boundaries typical of elongated dimeric molecules (Table I). As shown in Figure 6B, this fragment was partially active in the inhibition assay, demonstrating that a coiled-coil conformation of the binding site is required for the interaction with agrin.

To estimate the C-terminal border of the agrin-binding site, we prepared C-terminal deletion constructs from γ1_GΔN93AEΔC219 (Figure 6A). When these peptides were tested for inhibition (Figure 6B), only γ1_GΔN93AΔC3, γ1_GΔN93AΔC8 and γ1_GΔN93AΔC13 were partially effective, whereas γ1_GΔN93AΔC18, γ1_GΔN93AΔC23 and γ1_GΔN93AΔC28 showed no significant inhibition. Importantly, the GCN4 leucine zipper by itself did not interact with agrin (data not shown). Taken together, these results demonstrate that the agrin-binding site resides within a sequence comprising 20 residues (box in Figure 7A).

No significant agrin-binding activity of a laminin γ2 chimera

A comparison of the agrin-binding site of γ1 with known mammalian species and isoforms of laminin γ subunits is illustrated in the sequence alignment of Figure 7A. The agrin-binding sites of γ1 chains from mammals are 100% identical, whereas only a low degree of conservation is found between mouse γ1 and γ2 chains (55%), between human γ1 and γ2 chains

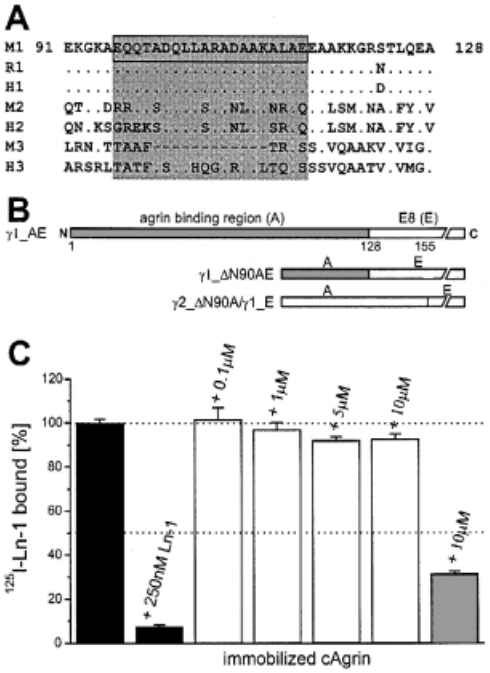

Fig. 7. Isoform specificity of agrin binding to laminin. (**A**) Sequence alignment of the agrin-binding site within the mouse laminin γ1 chain and other known mammalian γ sequences. The experimentally determined agrin-binding site comprises the boxed 20 residue sequence. Homologous sequences in laminin γ2 and γ3 chains are represented by the shaded area and conserved residues are indicated by dots. The mouse γ3 chain lacks 12 residues of our identified agrin-binding site, suggesting that the γ3 subunit of this species does not interact with agrin. M, mouse; R, rat; H, human. (**B**) Schematic representation of the chimeric γ2/γ1 fragment tested in the solid-phase radioligand-binding assay. (**C**) In contrast to unlabeled laminin-1 (black bars) and γ1_ΔN90AE (gray bars), no significant inhibition of the binding of 8 nM [^{125}I]laminin-1 to immobilized agrin was observed by the γ2_ΔN90A/γ1_E chimera (white bars). Values represent the mean ± SD of three measurements after subtraction of the background (BSA-coated wells). Background values were 2.3 ± 0.5% of total laminin-1 binding.

(45%), or between human γ1 and γ3 chains (35%). Interestingly, mouse γ3 lacks 12 residues of our identified agrin-binding site, suggesting that the γ3 subunit of this species does not interact with agrin.

In order to assess the agrin-binding property of the laminin γ2 chain, a chimeric protein, γ2_ΔN90A/γ1_E, was prepared that comprises a minimal γ2 sequence containing the potential agrin-binding site, fused to the coiled-coil-inducing E8 part from the γ1 subunit (Figure 7B). The degree of α-helicity, the thermal stability and the oligomerization state of the chimeric fragment as monitored by CD spectroscopy and analytical ultracentrifugation were similar to those of γ1_ΔN95AE (data not shown). However, the γ2_ΔN90A/γ1_E fragment, even at a concentration of 10 μM, did not inhibit the binding of iodinated laminin-1 to immobilized agrin (Figure 7C). This finding suggests that agrin binds selectively to specific laminin isoforms.

Discussion

Binding of agrin to the coiled-coil domain of laminin γ1

Several lines of evidence suggest that coiled-coil domains, in addition to their oligomerizing function, contain binding sites for other domains of the same or other proteins. Laminin-1 fragment E8, for example, contains sites that mediate interactions between cells and laminin (Deutzmann *et al*., 1992). Furthermore, peptides derived from the coiled-coil regions of single laminin subunits show binding to a variety of cell types (peptide Ile-Lys-Val-Ala-Val from α1 chain; Yamada, 1991) or were reported to inhibit outgrowth of motor neurons (peptide containing Leu-Arg-Glu from chicken β2 chain; Porter *et al*., 1995). We have reported recently that the three-stranded coiled-coil domain of laminin-1 binds to agrin (Denzer *et al*., 1998).

In this study, we have characterized the agrin-binding site in the coiled-coil domain of laminin-1 in detail. We have used both *in vivo* and *in vitro* experimental approaches to address whether one, two or all three chains of the heterotrimeric laminin-1 coiled coil are involved in the interaction with agrin. By performing binding studies with individual laminin-1 chains and recombinant coiled-coil fragments thereof, we found that the γ1 subunit is sufficient to mediate this interaction.

Our finding that the agrin-binding site resides within the laminin γ1 chain is supported further by the following unpublished observations. First, immunofluorescence studies revealed that interaction of agrin with full-length laminin-1 (Figure 2) was detected only in cells transfected with cDNA combinations containing the γ1 chain (e.g. γ1, α1/γ1, β1/γ1 and α1/β1/γ1), whereas no binding could be observed in cells transfected with α1, β1 or α1/β1 cDNAs. Furthermore, dose–response curves determined by solid-phase radioligand-binding assays yielded identical binding affinities of agrin for chick laminin-2 (chain combination: α2, β1 and γ1), chick laminin-4 (α2, β2 and γ1) and mouse laminin-1 (α1, β1 and γ1). As only the γ1 chain is common to all these isoforms of laminin, this subunit is likely to provide the amino acids essential for this interaction.

A coiled-coil conformation of the binding site is required for the interaction with agrin

Our findings demonstrate that although the γ1 chain is sufficient for the interaction with agrin, a coiled-coil structure of the agrin-binding site is required for the binding. The localization of the agrin-binding site within γ1 was assisted by the fact that recombinant γ1_AE-derived fragments tend to fold into weak homotypic coiled-coil structures that lack a unique chain stoichiometry (Figure 5; Table I). Intracellular immunofluorescence staining of COS cells transfected with γ1 cDNA (Figure 2) indicates that this weak interaction probably also occurs among full-length γ1 chains.

The presence of weak coiled-coil interactions among γ1_AE-derived fragments was supported further by solid-phase radioligand-binding assays of γ1_AE, γ1_A, γ1_GΔN93AEΔC219 and laminin-1 carried out at different temperatures (data not shown). The binding affinity of γ1_AE for agrin was increased at 4°C and significantly decreased at 37°C compared with 20°C. In contrast, the binding activities of γ1_GΔN93AEΔC219 and laminin-1, which fold into stable coiled-coil structures, did not vary significantly over this temperature range. As expected, the γ1_A peptide did not bind agrin significantly at any temperature tested.

The strongest evidence for a coiled-coil conformation of the binding site, however, is provided by the chimeric GCN4_γ1 fragments, in which the agrin-binding activity of inactive γ1 fragments has been rescued by in-register heptad repeat fusion to the GCN4 leucine zipper coiled coil (Figure 6A and B). The rather continuous loss of binding activity observed for the chimeric fragments (Figure 6A and B) may be understood in terms of weak cooperativity of the chimeric coiled coil. The CD thermal unfolding profile of the chimeric GCN4 fragment γ1_GΔN93AEΔC219 suggests that the dimeric fragments progressively melt from one or both ends. The shortest chimeric peptide, γ1_GΔN93AΔC13, which still showed agrin-binding activity, contains only 22 residues of the γ1 sequence and is almost identical to our identified agrin-binding site (Figure 7A). It should be emphasized that the chimeric GCN4_γ1 fragments were only used to delimit the C-terminal border of the agrin-binding site.

Clearly, the coiled-coil property of laminin chains by itself is not sufficient for an interaction with agrin. Although recombinant α1 and β1 polypeptide chain fragments, which are candidates for an agrin-binding site according to their electron microscopic localization (Denzer *et al*., 1998), fold into homotypic coiled-coil structures (Table I), no binding of these fragments to agrin was observed in competition and solid-phase binding assays. In addition, for the individual recombinant full-length α1 chain, there is electron microscopic-based evidence for a compact self-folded state of the coiled coil (Yurchenco *et al*., 1997). Clearly, no interaction of the recombinant full-length α1 chain with agrin was detected (Figure 2A).

Influence of the coiled-coil structure on the binding to agrin

A decrease in binding affinity of the recombinant γ1 chains and the chimeric GCN4 fusion proteins compared with native laminin-1 may be explained in terms of different coiled-coil structures in these molecules: the GCN4_γ1 chimera folds into homotypic coiled-coil dimers and the γ1_ΔN95AE fragments into a mixture of different oligomers, whereas the coiled-coil domain of native laminin-1 is a heterotrimer composed of α1, β1 and γ1 chains. A comparison of the crystal structures of wild-type and mutant GCN4 leucine zipper peptides has revealed that particular parameters, such as the supercoil radius (4.9 Å in the dimer versus 6.7 Å in the trimer) and the supercoil pitch (148 Å in the dimer versus 175 Å in the trimer), differ markedly between two- and three-stranded coiled coils (O'Shea *et al*., 1991; Harbury *et al*., 1994). In addition, these parameters can vary significantly between different coiled-coils of the same oligomerization state (see Tao *et al*., 1997). Consequently, the conformation of the binding site in the chimeric GCN4_γ1 fragments and the fragments derived from γ1_ΔN95AE may be similar but not identical to that in the native laminin-1 coiled-coil heterotrimer. It is conceivable that α1 and β1 chains may have a supporting structural function and may provide the coiled-coil framework necessary for high-affinity binding to agrin, although they alone are not sufficient for the interaction with agrin. However, we can not exclude that single side chains of α1 and β1 chains contribute to agrin binding, although the main binding site resides within the γ1 chain. We conclude that structural differences between the native molecule and the recombinant fragments account for the decrease in binding affinity.

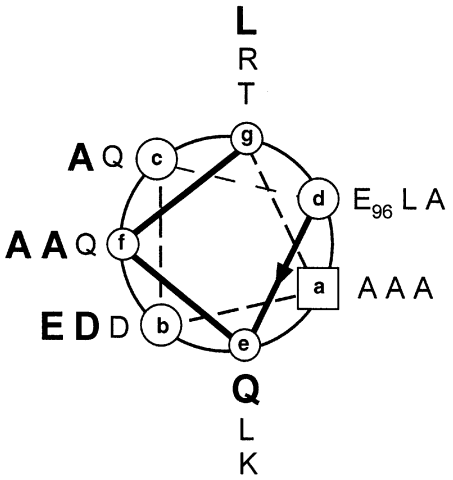

Fig. 8. Helical wheel representation of residues comprising the agrin-binding site. The sequence starts with Glu96 (Glu1296; Sasaki and Yamada, 1987) in a heptad **d** position and ends with Glu115 (Glu1315) in a heptad **b** position. View is from the N-terminus, and heptad repeat positions are labeled **a**–**g**. The seven surface-exposed residues of the γ1 chain that are not conserved in the γ2 chain are indicated in bold.

Residues potentially involved in the interaction with agrin

With the exception of the residues at heptad positions **a** and **d**, which form the hydrophobic core of a coiled coil, all the other residues are surface exposed and therefore possibly involved in contacts with other proteins. The seven surface-exposed residues of the binding site that are not conserved in the inactive homologous γ2 sequence (Figure 7) are candidate residues for the interaction with agrin. Of these, Gln97 (Gln1297; Sasaki and Yamada, 1987) is particularly interesting because it is contained in the shortest N-terminal fragment that still shows agrin-binding activity. In the γ2 chain, this position is occupied by a charged Arg residue. A helical wheel projection of the residues of the agrin-binding site reveals that hydrophobic and polar γ1-specific residues fall on separate sides of the coiled-coil α-helix surface (Figure 8). Notably, such stripes of residues ideally could interact with a groove in the NtA domain of agrin. With the help of the recently solved crystal structure of the NtA domain at 1.6 Å resolution (J.Stetefeld, J.Engel and R.A.Kammerer, in preparation), characterization of the laminin-1–agrin interaction now appears feasible in atomic detail.

Distribution of laminin γ chains

To date, 12 laminin isoforms have been characterized (i.e. laminin-1 to -12; Miner *et al*., 1997, and references therein; Koch *et al*., 1999), and more are expected to exist. Ten of these isoforms contain the γ1 chain. Laminin-5 is the only isoform composed of the γ2 subunit (Kallunki *et al*., 1992) and laminin-12 contains the recently described γ3 chain (Koch *et al*., 1999). Based on our finding that the agrin-binding site resides within the γ1 chain, agrin is expected to bind to 10 of these laminin isoforms.

The tissue distribution of the three laminin γ chains differs markedly. Whereas the γ1 subunit shows a widespread distribution in all cellular basement membranes, the γ2 and γ3 chains are restricted predominantly to the dermal–epidermal junction of the skin (Rousselle *et al*., 1991) and to nerve-associated, non-basement membrane structures of different locations in the brain (Koch *et al*., 1999), respectively. It is not known whether agrin co-localizes with the laminin γ2 and γ3 chains. However, the presence of agrin in several distinct basement membranes indicates a co-distribution with laminin isoforms containing the γ1 subunit. Taken together, our findings support the notion that laminin isoforms play an important role in the distinct molecular composition of basement membranes.

Materials and methods

Construction of expression plasmids

Constructs pcAgrin and pcN25Fc are described elsewhere (Denzer *et al*., 1995, 1997). The full-length cDNA constructs encoding the α1, β1 and γ1 subunits of mouse laminin-1 are described by Yurchenco *et al*. (1997).

cDNA inserts for the expression of the recombinant mouse α1_AE (residues Leu1767–Gln2133), β1_AE (Leu1412–Leu1765) and γ1_AE (Tyr1201–Pro1574) laminin polypeptide chain fragments (for numbering, refer to Sasaki and Yamada, 1987; Sasaki *et al*., 1987, 1988) were prepared from the published cDNA clones (Sasaki and Yamada, 1987; Sasaki *et al*., 1987, 1988) by PCR using *Pfu* DNA polymerase (Stratagene). Specific primers were designed to obtain an *Nde*I site at the 5′ end and two TAA translation stop codons followed by a *Bam*HI at the 3′ end. The amplified products were ligated into the *Nde*I–*Bam*HI site of the bacterial expression vector pET-15 (Novagen).

γ1_AE was used to prepare the N-terminal γ1 deletion constructs γ1_ΔN50AE (from Ala1251), γ1_ΔN60AE (Leu1261), γ1_ΔN70AE (Asp1271), γ1_ΔN80AE (Gly1281), γ1_ΔN90AE (Glu1291), γ1_ΔN95AE (Glu1296), γ1_ΔN100AE (Asp1301), γ1_ΔN105AE (Arg1306), γ1_ΔN110AE (Lys1311), γ1_ΔN120AE (Gly1321) and γ1_E (Asn1329). Sense primers were designed to contain an *Nde*I site at the 5′ end and antisense primers were designed to span unique *Xho*I or *Eco*RI restriction sites within γ1_AE. For all PCR experiments, Ampli-Taq DNA polymerase (Roche Molecular Systems) was used. Subsequently, the original *Nde*I–*Xho*I or *Nde*I–*Eco*RI fragments of γ1_AE were replaced by the PCR products, yielding the N-terminally truncated γ1 fragments. For the *Nde*I–*Eco*RI constructs, a pET-15b variant was used in which the original *Eco*RI site of the vector had been removed by DNA fill-in synthesis.

Mouse cDNA (Sasaki and Yamada, 1987; Sasaki *et al*., 1987, 1988) was used as a template for the PCR amplification of DNA fragments encoding peptides α1_A (residues Leu1767–Ala1886), β1_A (Leu1412–Ile1539) and γ1_A (Tyr1201–Ala1328) of the agrin-binding region. Primer sets were used that introduce a *Bam*HI site at the 5′ end and two TAA translation stop codons and an *Eco*RI site at the 3′ end. In addition, β1_A and γ1_A were designed to contain a C-terminal Gly-Gly-Cys linker sequence. The amplified products were ligated into the bacterial expression vector pPEP-T (Kammerer *et al*., 1998a) at *Bam*HI–*Eco*RI sites.

The designed chimeric polypeptide chain fragment γ1_GΔN93A-EΔC219 [Met2–Val30 of the GCN4 leucine zipper GCN4p-wt peptide (Kammerer *et al*., 1998b) joined in-heptad repeat register to the N-terminus of Lys1294–Ile1356 of γ1] was generated by the gene splicing method described by Horton *et al*. (1989). Specific oligonucleotides were designed to obtain a *Bam*HI site at the 5′ end and two TAA translation stop codons and an *Eco*RI at the 3′ end.

γ1_GΔN93AEΔC219 was used for the construction of the C-terminally truncated chimeras γ1_GΔN93AΔC3 (to Leu1325), γ1_GΔN93AΔC8 (Lys1320), γ1_GΔN93AΔC13 (Glu1315), γ1_GΔN93AΔC18 (Ala1310), γ1_GΔN93AΔC23 (Ala1305) and γ1_GΔN93AΔC28 (Ala1300). For PCR amplification, the sense primer for the generation of γ1_GΔN-93AEΔC219 and antisense primers containing two TAA translation stop codons followed by an *Eco*RI site were used. The PCR products were ligated into the *Bam*HI–*Eco*RI site of pPEP-T.

The chimeric polypeptide chain fragment γ2_ΔN90A/γ1_E was constructed from γ1_AE. A DNA fragment encoding the mouse γ2 sequence corresponding to the homologous sequence in γ1 (Glu1291–Arg1354) was amplified by PCR from a randomly primed mouse keratinocyte cDNA library. Specific primers were used to obtain an *Nde*I site at the 5′ end and the authentic *Eco*RI site of γ1_AE at the 3′ end. Subsequently, the original *Nde*I–*Eco*RI fragment of γ1_AE was replaced by the PCR product, yielding the chimeric construct in the above-mentioned pET-15b vector.

PCR and DNA manipulations for cloning were performed according to standard protocols. All constructs were verified by DNA sequencing.

Expression and purification of recombinant polypeptide chain fragments

The full-length laminin-1 chains were expressed transiently in transfected COS-7 cells. The intracellular pool of laminin subunits was examined by lysing the transfected cells with SDS–PAGE sample buffer and subjecting the total extract to Western blot analysis using the anti-laminin antibody 143 (Aeschlimann and Paulsson, 1991) as described in detail by Denzer *et al*. (1995). The recombinant proteins cAgrin and cN25Fc were purified from conditioned medium of stably transfected HEK 293 and transiently transfected COS-7 cells as described by Denzer *et al*. (1998). Mouse laminin-1 was purified from mouse Engelbreth–Holm–Swarm sarcoma according to Timpl *et al*. (1979).

The *E.coli* JM109(DE3) host strain (Promega) was used for all bacterial expression experiments. Production and purification of His_6-tagged fusion proteins by immobilized metal affinity chromatography on Ni^{2+}–Sepharose (Novagen) was performed under denaturing conditions as described in the manufacturer's instructions. Separation of recombinant polypeptide chain fragments from the His_6 tag (pET-15b constructs) or the His_6-tagged carrier protein (pPEP-T constructs) by thrombin cleavage was carried out as described by Kammerer *et al*. (1998a). Recombinant polypeptide chain fragments were dialyzed against 5 mM sodium phosphate buffer (pH 7.4) supplemented with 150 mM sodium chloride and stored at –20°C. For α1_AE, the addition of 1 M urea was necessary to prevent precipitation. Alkylation of polypeptide chains by *N*-ethylmaleimide was performed as described by Denzer *et al*. (1998). Concentrations of bacterially expressed proteins were determined by tyrosine absorbance in 6 M GuHCl (Edelhoch, 1967) or the BCA assay (Pierce).

Solid-phase radioligand-binding assay

Iodination of laminin-1 was performed as described by Denzer *et al*. (1997). cAgrin was diluted to 2.5–5 μg/ml with 50 mM sodium bicarbonate (pH 9.6) and immobilized on microtiter plates (Becton Dickinson) by overnight incubation at 4°C. Remaining binding sites were blocked for 1 h with Tris-buffered saline (TBS) (pH 7.4) containing 3% bovine serum albumin (BSA) and 10 mM EDTA (blocking solution). Iodinated laminin-1 diluted in blocking solution was added and incubated for 2 h at room temperature. At this step, the recombinant laminin chain fragments were included as competitors. After washing four times with TBS (pH 7.4) containing 10 mM EDTA, radioactivity in each well was counted with a gamma counter.

Intracellular binding assay

COS-7 cells transiently transfected with cDNAs encoding individual laminin-1 subunits were processed for intracellular protein staining as follows: after washing with phosphate-buffered saline (PBS), the cells were fixed for 30 min at room temperature with 4% paraformaldehyde, 11% sucrose in 0.1 M potassium phosphate buffer (pH 7.2). After rinsing with PBS and 20 mM glycine in PBS, cells were permeabilized with 0.1% saponin in PBS (PBSS). cN25Fc (45 nM) in PBSS containing 10% horse serum was incubated for 2 h at room temperature. At this step, γ1_AE was added as competitor to a final concentration of 10 μM. After four washes with PBSS, cells were incubated for 1 h at room temperature with biotinylated horse anti-mouse IgG (5 μg/ml; Vector Laboratories, Inc.), followed by a 1 h incubation at room temperature with Cy3-conjugated streptavidin (2 μg/ml; Jackson ImmunoResearch Laboratories, Inc.). After washing, cultures were mounted on glass coverslips with citifluor and examined with a microscope equipped for epifluorescence (Leica, Inc.).

CD spectroscopy

Analysis of the recombinant polypeptide chain fragments was performed as described by Kammerer *et al*. (1998a).

Analytical ultracentrifugation

Sedimentation equilibrium and sedimentation velocity experiments were performed at 20°C on a Beckman Optima XL-A analytical ultracentrifuge

equipped with 4 and/or 12 mm Epon double-sector cells in an An-60 Ti rotor. Recombinant polypeptide chain fragments were analyzed in 5 mM sodium phosphate buffer (pH 7.4) supplemented with 150 mM sodium chloride with protein concentrations adjusted to 0.25–1.2 mg/ml. Sedimentation velocity runs were performed at rotor speeds of 56 000 r.p.m. Sedimenting material was assayed by its absorbance at 234 or 278 nm. Sedimentation coefficients were corrected to standard conditions (water, 20°C) (van Holde, 1985). Sedimentation equilibrium scans were carried out at 16 000–32 000 r.p.m. depending on the molecular mass. Average molecular masses were evaluated by the best linear fit of ln$A$ versus r^2, where A is the absorbance and r the distance from the rotor center (van Holde, 1985). A partial specific volume of 0.73 ml/g was used for all calculations.

Acknowledgements

We are especially indebted to Dr M.Koch (Harvard Medical School) for the gift of randomly primed keratinocyte cDNAs. We thank Dr C.-A.Schoenenberger for critical reading of the manuscript. This work was supported by grants from the Swiss National Science Foundation.

References

Aeschlimann,D. and Paulsson,M. (1991) Cross-linking of laminin–nidogen complexes by tissue transglutaminase. A novel mechanism for basement membrane stabilization. *J. Biol. Chem.*, **266**, 15308–15317.

Alber,T. (1992) Structure of the leucine zipper. *Curr. Opin. Genet. Dev.*, **2**, 205–210.

Bork,P. and Bairoch,A. (1995) Extracellular protein modules: a proposed nomenclature. *Trends Biochem. Sci. (Suppl.)*, **20**, 104–105.

Clark,E.A. and Brugge,J.S. (1995) Integrins and signal transduction pathways: the road taken. *Science*, **268**, 233–239.

Cohen,C. and Parry,D.A.D. (1990) α-Helical coiled coils and bundles: how to design an α-helical protein. *Proteins*, **7**, 1–15.

Crick,F.H.C. (1953) The packing of α-helices: simple coiled-coils. *Acta Crystallogr.*, **6**, 689–697.

Denzer,A.J., Gesemann,M., Schumacher,B. and Ruegg,M.A. (1995) An amino-terminal extension is required for the secretion of chick agrin and its binding to extracellular matrix. *J. Cell Biol.*, **131**, 1547–1560.

Denzer,A.J., Gesemann,M. and Ruegg,M.A. (1996) Diverse functions of the extracellular matrix molecule agrin. *Semin. Neurosci.*, **8**, 357–366.

Denzer,A.J., Brandenberger,R., Gesemann,M., Chiquet,M. and Ruegg,M.A. (1997) Agrin binds to the nerve–muscle basal lamina via laminin. *J. Cell Biol.*, **137**, 671–683.

Denzer,A.J., Schulthess,T., Fauser,C., Schumacher,B., Kammerer,R.A., Engel,J and Ruegg,M.A. (1998) Electron microscopic structure of agrin and mapping of its binding site in laminin-1. *EMBO J.*, **17**, 335–343.

Deutzmann,R., Aumailley,M., Wiedemann,H., Pysny,W., Timpl,R. and Edgar,D. (1990) Cell adhesion, spreading and neurite stimulation by laminin fragment E8 depends on maintenance of secondary and tertiary structure in its rod and globular domain. *Eur. J. Biochem.*, **191**, 513–522.

Edelhoch,H. (1967) Spectroscopic determination of tryptophan and tyrosine in proteins. *Biochemistry*, **6**, 1948–1954.

Harbury,P.B., Kim,P.S. and Alber,T. (1994) Crystal structure of an isoleucine-zipper trimer. *Nature*, **371**, 80–83.

Henry,M.D. and Campbell,K.P (1996) Dystroglycan: an extracellular matrix receptor linked to the cytoskeleton. *Curr. Opin. Cell Biol.*, **8**, 625–631.

Horton,R.M., Hunt,H.D., Ho,S.N., Pullen,J.K. and Pease,L.R. (1989) Engineering hybrid genes without the use of restriction enzymes: gene splicing by overlap extension. *Gene*, **77**, 61–68.

Kallunki,P. *et al*. (1992) A truncated laminin chain homologous to the B2 chain: structure, spatial expression, and chromosomal assignment. *J. Cell Biol.*, **119**, 679–693.

Kammerer,R.A. (1997) α-Helical coiled-coil oligomerization domains in extracellular proteins. *Matrix Biol.*, **15**, 555–565.

Kammerer,R.A., Schulthess,T., Landwehr,R., Lustig,A., Fischer,D. and Engel,J. (1998a) Tenascin-C hexabrachion assembly is a sequential two-step process initiated by coiled-coil α-helices. *J. Biol. Chem.*, **273**, 10602–10608.

Kammerer,R.A., Schulthess,T., Landwehr,R., Lustig,A., Engel,J., Aebi,U. and Steinmetz,M.O. (1998b) An autonomous folding unit mediates the assembly of two-stranded coiled coils. *Proc. Natl Acad. Sci. USA*, **95**, 13419–13424.

Koch,M., Olson,P.F., Albus,A., Jin,W., Hunter,D.D., Brunken,W.J., Burgeson,R.E. and Champliaud,M.F. (1999) Characterization and expression of the laminin γ3 chain: a novel, non-basement membrane-associated, laminin chain. *J. Cell Biol.*, **145**, 605–618.

Landschulz,W.H., Johnson,P.F. and McKnight,S.L. (1988) The leucine zipper: a hypothetical structure common to a new class of DNA binding proteins. *Science*, **240**, 1759–1764.

Lupas,A. (1996) Coiled coils: new structures and new functions. *Trends Biochem. Sci.*, **21**, 375–382.

Maurer,P. and Engel,J. (1996) Structure of laminins and their chain assembly. In Ekblom,P. and Timpl,R. (eds), *The Laminins*. Harwood Academic Publishers, The Netherlands, pp. 27–49.

McLachlan,A.D. and Stewart,M. (1975) Tropomyosin coiled-coil interactions: evidence for an unstaggered structure. *J. Mol. Biol.*, **98**, 293–304.

McMahan,U.J. (1990) The agrin hypothesis. *Cold Spring Harb. Symp. Quant. Biol.*, **55**, 407–418.

Miner,J.H., Patton,B.L., Lentz,S.I, Gilbert,D.J., Snider,W.D., Jenkins,N.A., Copeland,N.G. and Sanes,J.R. (1997) The laminin α chains: expression, developmental transitions, and chromosomal locations of α1-5, identification of heterotrimeric laminins 8–11, and cloning of a novel α3 isoform. *J. Cell Biol.*, **137**, 685–701.

O'Shea,E.K., Klemm,J.D., Kim,P.S. and Alber,T. (1991) X-ray structure of the GCN4 leucine zipper, a two-stranded, parallel coiled coil. *Science*, **254**, 539–544.

Porter,B.E., Weis,J. and Sanes,J.R. (1995) A motoneuron-selective stop signal in the synaptic protein S-laminin. *Neuron*, **14**, 549–559.

Rousselle,P., Lunstrum,G.P., Keene,D.R. and Burgeson,R.E. (1991) Kalinin: an epithelium-specific basement membrane adhesion molecule that is a component of anchoring filaments. *J. Cell Biol.*, **114**, 567–576.

Sasaki,M. and Yamada,Y. (1987) The laminin B2 chain has a multidomain structure homologous to the B1 chain. *J. Biol. Chem.*, **262**, 17111–17117.

Sasaki,M., Kato,S., Kohno,K., Martin,G.R. and Yamada,Y. (1987) Sequence of the cDNA encoding the laminin B1 chain reveals a multidomain protein containing cysteine-rich repeats. *Proc. Natl Acad. Sci. USA*, **84**, 935–939.

Sasaki,M., Kleinman,H.K., Huber,H., Deutzmann,R. and Yamada,Y. (1988) Laminin, a multidomain protein. The A chain has a unique globular domain and homology with the basement membrane proteoglycan and the B chains. *J. Biol. Chem.*, **263**, 16536–16544.

Sodek,J., Hodges,R.S., Smillie,L.B. and Jurasek,L. (1972) Amino-acid sequence of rabbit skeletal tropomyosin and its coiled-coil structure. *Proc. Natl Acad. Sci. USA*, **69**, 3800–3804.

Tao,Y., Strelkov,S.V., Mesyanzhinov,V.V. and Rossmann,M.G. (1997) Structure of bacteriophage T4 fibritin: a segmented coiled coil and the role of the C-terminal domain. *Structure*, **5**, 789–798.

Timpl,R. and Brown,J.C. (1994) The laminins. *Matrix Biol.*, **14**, 275–281.

Timpl,R., Rohde,H., Robey,P.G., Rennard,S.I., Foidart,J.M. and Martin,G.R. (1979) Laminin—a glycoprotein from basement membranes. *J. Biol. Chem.*, **254**, 9933–9937.

van Holde,K.E. (1985) *Physical Biochemistry.* 2nd edn. Prentice Hall, Englewood Cliffs, NJ, pp. 93–136.

Yamada,K.M. (1991) Adhesive recognition sequences. *J. Biol. Chem.*, **266**, 12809–12812.

Yurchenco,P.D. and Cheng,Y.S. (1993) Self-assembly and calcium-binding sites in laminin: a three-arm interaction model. *J. Biol. Chem.*, **268**, 17286–17299.

Yurchenco,P.D. and O'Rear,J.J. (1994) Basal lamina assembly. *Curr. Opin. Cell Biol.*, **6**, 674–681.

Yurchenco,P.D., Quan,Y., Colognato,H., Mathus,T., Harrison,D., Yamada,Y. and O'Rear,J.J. (1997) The α chain of laminin-1 is independently secreted and drives secretion of its β- and γ-chain partners. *Proc. Natl Acad. Sci. USA*, **94**, 10189–10194.

Received June 30, 1999; revised September 21, 1999; accepted October 4, 1999